International Journal of Creative and Open Research in Engineering and Management
ISSN: **3108-1754 (Online)**
Volume 02 Issue 05 May-2026 | Impact Factor: 3.5

IOT Monitored Variable Frequency Drive (VFD) Based 3 Phase Induction Motor Control System

Dr. P. G. Asutkar, Aditya R. Shende, Taral B. Deogade, Vedant V. Nawale, Snehal R. Karmarkar, Vaibhav V. Pogulwar, Tushar R. Karmarkar

Assistant Professor, Electrical Engineering Department, Rajiv Gandhi College of Engineering, Research & Technology, Chandrapur

Studemts of Electrical Engineering Department, Rajiv Gandhi College of Engineering, Research & Technology, Chandrapur

How to Cite this Article:
Shende, A. R., Deogade, T. B., Nawale, V. V., Karmarkar, S. R., Pogulwar, V. V. & Karmarkar, T. R. (2026). IOT Monitored Variable Frequency Drive (VFD) Based 3 Phase Induction Motor Control System. International Journal of Creative and Open Research in Engineering and Management, <i>02</i>(05). https://doi.org/10.55041/ijcope.v2i5.821

https://doi.org/ 10.55041/ijcope.v2i5.821

Abstract

This paper presents the design, development, and experimental validation of an intelligent, cost-effective, and Internet of Things (IoT)-enabled Variable Frequency Drive (VFD) control framework for three-phase induction motors. Utilizing a high-performance PIC18F25K22 microcontroller as the localized processing engine, the system achieves granular speed modulation by driving a Lenze AC Tech SMVector VFD via a highly precise 0-10V analog reference signal. This reference voltage was generated using an external MCP4922 12-bit Digital-to-Analog Converter (DAC) operating over the Serial Peripheral Interface (SPI) protocol, minimizing the CPU overhead and eliminating analog calibration drifts. Real-time ambient environmental tracking was achieved using a calibrated SHT40I sensor array, providing automated, threshold-triggered speed scaling to safeguard electrical enclosures from thermal stress. Operational telemetry, encompassing motor state, temperature, humidity, and drive duty cycles, is serialized over a Universal Asynchronous Receiver-Transmitter (UART) interface, establishing seamless integration with edge devices, virtual COM ports, and cloud platforms via Node-RED dashboards. The experimental findings demonstrate a maximum DAC absolute voltage error within ± 0.2% and highly stable data-logging capabilities. The proposed framework provides a robust, scalable, and low-cost decentralized alternative to conventional PLC-SCADA architectures, in alignment with modern Industry 4.0 paradigms.

Keywords—Variable Frequency Drive (VFD), Three-Phase Induction Motor, PIC18F25K22, MCP4922, IoT Telemetry, Industrial Automation, Smart Enclosures.

1. Introduction

Three-phase induction motors are the foundational workhorses of modern industrial infrastructure, constituting more than 70% of rotating machinery deployments and consuming approximately 45–50% of global electrical energy. Consequently, optimizing their speed profiles and runtime efficiencies is a critical objective in industrial automation and energy management systems. Traditional starting methodologies, such as direct-on-line (DOL) or star-delta switching, generate severe transient inrush currents and abrupt mechanical stresses, which reduce the motor insulation lifespan and degrade the power quality of the networks. Although contemporary Variable Frequency Drives (VFDs) mitigate these deficiencies through voltage-to-frequency (V/f) scaling, standard commercial VFD deployments operate as closed, standalone systems. They often lack integrated environmental monitoring, localized low-cost computing intelligence, and native Internet of Things (IoT) connectivity, which are necessary for remote diagnostic orchestration and predictive maintenance.

This study details a cost-effective, multi-peripheral embedded platform that introduces real-time environmental awareness and remote IoT telemetry into industrial motor control circuits. By shifting command execution from expensive Programmable Logic Controllers (PLCs) to an optimized 8-bit microcontroller framework, the system achieves high economic scalability while maintaining strict industrial reliability. The core computing unit manages concurrent communication lines, including an SPI bus for driving a high-resolution 12-bit DAC speed reference, discrete general-purpose input/output (GPIO) pins for galvanic isolation relays, and a high-speed UART module for wireless localized or global IoT data logging. The integration of these features enables multi-tiered safety control loop execution, wherein the system dynamically rescales the motor speeds under critical thermal or ambient variations.

2. Literature Review

The design of modern alternating current (AC) motor drives can be traced back to the pioneering field-oriented control (FOC) framework established by Blaschke, which mathematically decouples stator currents into decoupled torque- and flux-producing vector components. Subsequent advancements in space vector pulse width modulation (SVPWM) have enabled advanced VFDs to implement scalar or vector control mechanisms with reduced harmonic profiles. As documented by Bose, modulating motor speeds in variable-torque loads (such as centrifugal fans or industrial pumps) according to the fluid affinity laws yields substantial energy savings. These reductions are governed by the relationship, where the power consumption scales cubically with the rotational speed:

$$\mathbf{P} \propto N^3$$

where P represents the active power consumed and N denotes the shaft rotational speed.

Traditional industrial configurations interface VFDs with supervisory networks using PLC modules. However, recent literature indicates an explicit pivot toward embedded microcontroller deployments because of their modularity and lower deployment barriers. Garcia et al. verified that mid-range microcontrollers can manage VFD acceleration and deceleration scaling efficiently across specific industrial load profiles. To resolve speed stepping granularities associated with standard microcontroller pulse-width modulation (PWM) low-pass filtering, Huang and Chen highlighted that external SPI-driven Digital-to-Analog Converters (DACs) significantly reduce CPU computational delays while generating smooth linear control inputs.

Simultaneously, contemporary architectural upgrades require the implementation of cloud-connected frameworks. Marzuki et al. demonstrated a low-cost, Modbus RTU interface pairing an ESP32 master with a VFD network to provide global diagnostic access over web platforms. Similarly, Buwarda et al. developed localized automation models using ambient thermal telemetry to scale Altivar drives in discrete steps. However, these steps lack a linear adjustment resolution. This study addresses these identified research gaps by presenting a continuous, high-resolution, linear analog tracking drive that seamlessly pairs predictive environmental telemetry with uninterrupted UART/Bluetooth telemetry.

Title	**Method Used**	**Key Findings**	**Limitations**
Integrated Real-Time Monitoring of Three-Phase Induction Motors *Authors: M. M. Siddiqui, A. S. A. Hadhri, A. S. H. A. Kathir, A. A. Alnajjar*	Real-time monitoring using sensors and data acquisition systems.	Developed a system for continuous monitoring of motor parameters improving fault detection and operational efficiency.	Limited real-world industrial validation; scalability not discussed.
Induction Motors with Variable Frequency Drives: A Systematic Review with Focus on Health Monitoring *Authors: P. Shaw, N. K. Sharma, B. Patnaik*	Review of VFD-based systems and health monitoring techniques.	Highlighted importance of VFD integration with predictive maintenance and condition monitoring.	Being a review paper, lacks experimental implementation and quantitative results.
Three-phase induction motor control using scalar control method based on IoT *Author : N. R. Putri, M. Yuhendri*	Scalar control (V/f control) integrated with IoT platform	Demonstrated remote monitoring and control of motor using IoT with stable performance	Scalar control has lower dynamic performance compared to vector control; limited precision
Design and Development of a Three-Phase Induction Motor Speed Control System Using Altivar 61 Based on Temperature Sensor and IoT *Authors: S. Buwarda, Mutmainnah, M. F. Yakob*	VFD (Altivar 61) with temperature sensors and IoT integration	Achieved efficient speed control and temperature-based protection with remote monitoring	Focus limited to temperature parameter; other fault parameters not considered

Advanced Control and Protection of Three-Phase Induction Motors for Industrial Automation *Author : G. Anbarasi*	Advanced control techniques with protection schemes (likely PLC/automation-based)	Enhanced motor safety and performance in industrial automation environments	Lack of detailed experimental validation and real-time deployment results

Proposed System

The conceptual architecture of the proposed industrial automation platform relies on a modular embedded framework designed to execute sensor data acquisition, precision reference signal generation, and bidirectional network telemetry concurrently.

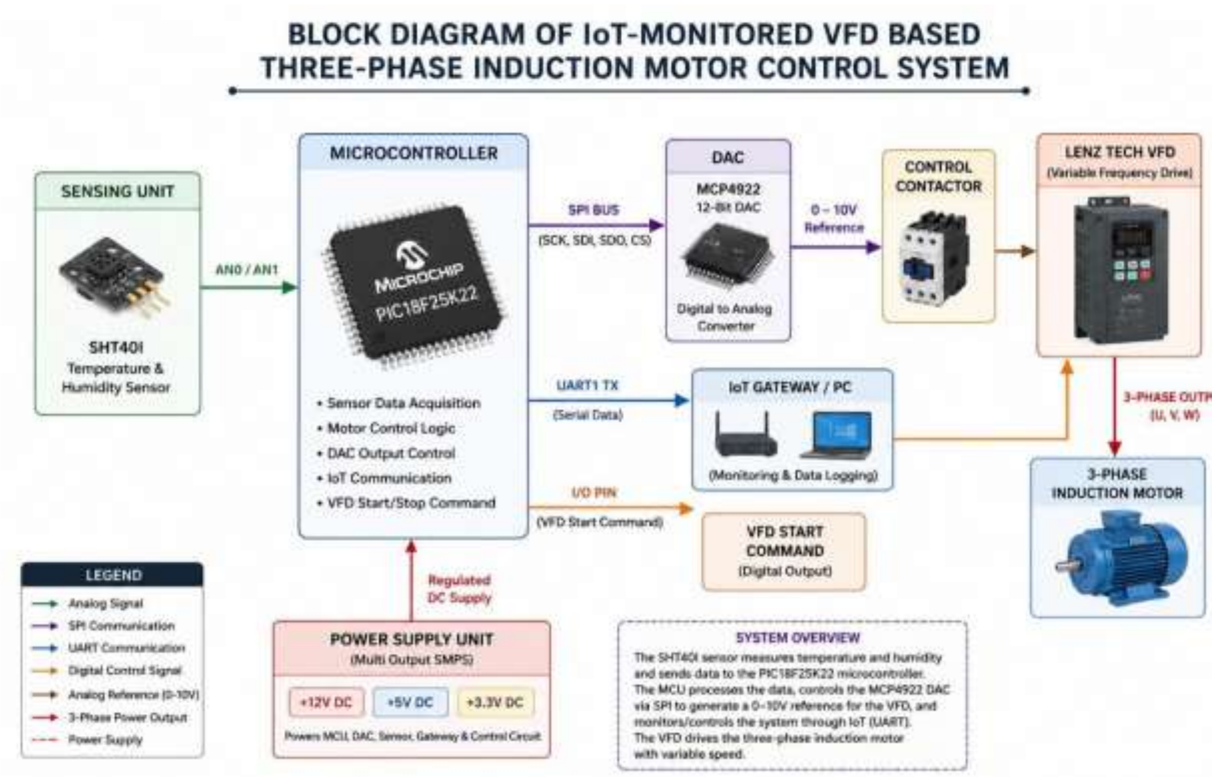

Figure 3.1: Block Diagram of The System

The system operates via sequential functional stages:

1. **Environmental Sensing:** The ambient state of the industrial enclosure or immediate motor housing is continuously read via the analog channels of the microcontroller. This configuration prevents communication blockages on the internal bus lines while supporting rapid and deterministic sampling cycles.

2. **Centralized Processing:** A central processing unit executes the main control loop. It filters raw sensor data, formats ASCII output telemetry strings, assesses safety operational boundaries, and maps speed percentages to digital control bits.

3. **Precision Analog Interface:** The computed speed profile is transmitted over an SPI data stream to a standalone 12-bit DAC. The native voltage output is structurally scaled via an instrumentation operational amplifier to match the standard industrial VFD specifications (0-10 VDC).

4. **Galvanic Control & Isolation:** High-voltage initialization sequences are safely separated from the logic electronics through an NPN-driven electromechanical contactor arrangement, shielding the digital sub-systems from inductive voltage spikes.

5. **Edge/Cloud Visualization:** Transmitted data fields are translated via edge interfaces to populated software dashboards, updating operators on status trends and triggering anomalies.

3. System Architecture and Design

A. Hardware Subsystems

The physical infrastructure is partitioned into designated functional nodes to guarantee optimal operational stability and noise immunity under industrial conditions.

1. **Microcontroller Node:** The core computation engine is the 8-bit PIC18F25K22 microcontroller. Operating at an internal clock frequency of 16 MHz uprated via an internal Phase-Locked Loop (PLL) multiplier to 64 MHz, it yields an execution rate of 16 million instructions per second (MIPS). The hardware includes dual Master Synchronous Serial Port (MSSP) blocks configured for high-speed SPI , alongside enhanced EUSART engines for serial telemetry strings.

2. **Digital-to-Analog Converter (DAC):** The system integrates an MCP4922 dual-channel 12-bit voltage output DAC. It processes serial commands over the hardware SPI link at speeds of up to 20 MHz. Channel A generates an output voltage spanning 0 (5V) across 4096 discrete steps, achieving high stability and an Integral Non-Linearity (INL) within the LSB.

3. **Variable Frequency Drive Hardware:** Speed modulation was executed using an industrial Lenze AC Tech SMVector (SMV series) inverter rated for a 5.0 HP (4.0 kW) output footprint. The drive accepts input lines of 3-phase 400/480 VAC and runs in an enhanced sensorless vector control mode to maintain constant torque trajectories across a linear frequency band of 0 – 500 Hz.

4. **Three-Phase Induction Motor:** The structural load consists of a rugged squirrel-cage induction motor rated at 1.5 kW (2.0 HP) with a baseline full-load rotational speed of 1400 RPM at 415 V/ 50 Hz.

5. **Environmental Sensing Node:** Localized parameter ingestion uses a modified SHT40I module, providing a linear analog voltage output ranging from 0.5 – 4.5 V mapped proportionally across specified limits. Channel AN0 maps the temperature from -40 to +125 °C , whereas AN1 records the relative humidity from 0 to 100%.

Component Feature	Core Operational Parameters and Technical Specifications
PIC18F25K22 MCU	32KB Flash, 1536 B SPRAM, 64MHz Clock, Dual EUSART, 10-bit ADC
MCP4922 DAC	12-bit resolution, 2 Channels, SPI Interfacing up to 20 MHz, INL 1 LSB max.
Lenze AC Tech VFD	3-Phase 400/480 V, 5.0 HP Output, Dual Analog Input (0-10 V / 4 – 20 mA), 0.01 Hz Resolution.
Induction Motor	Squirrel-Cage Type, 1.5 kW Power, 1400 RPM, 3.3A at Full Load Current, Class B Insulation.
SHT40I Sensor Module	Temperature Range: -40 to +125 °C, humidity Range: 0-100% RH, 0.2 °C temperature accuracy.

B. Signal Conditioning and Power Routing

To operate reliably in noisy industrial environments alongside high-power switching circuits, the system integrates specialized signal conditioning and protection subcircuits.

Amplification Circuitry: Because the MCP4922 DAC outputs a maximum of 5V under a standard 5V supply, an LM324 operational amplifier was integrated into a non-inverting gain configuration = 2.0). This linearly transforms the signal to the standard industrial 0-10 V reference scale required by the VFD terminal.

Power Rail Segmentation: A multi-rail Switch-Mode Power Supply (SMPS) delivers segmented DC voltages. A 12 VDC line powers the analog operational amplifiers and relay actuator coils, an intermediate 5 VDC rail powers the signaling LEDs, and a low-dropout LM1117-3.3 regulator provides a quiet 3.3 VDC rail for the core logic processors and Bluetooth telemetry nodes.

Transient Suppression Elements: High-voltage inductive transients are managed using 1N4007 flyback diodes connected in anti-parallel configurations across the inductive relay coils to safeguard the driver transistors. Reverse polarity safety is handled by a heavy-duty 1N5408 diode at the master input stage, whereas a metal-oxide varistor (MOV) clamps the primary AC line voltage surges.

4. Implementation

A. Mathematical Modeling and Peripheral Interfacing

The translation of software setpoints into motor rotational speeds requires linear-scaling models across successive hardware domains. The target speed percentage (S% bounded between 0.0 and 100.0) is mapped directly to a 12-bit digital value () according to the following mapping equation:

$$D_{DAC} = \left[\frac{S\,\%}{100.0} \times 4095 \right]$$

The voltage output (V_{out_DAC}) generated by the MCP4922 converter node is a function of its voltage reference (V_{REF} = 5.0 V) and configuration bits:

$$V_{out\_DAC} = \left[\frac{D_{DAC}}{100.0} \times 4095 \right]$$

The Passage through the LM324 non-inverting scaling stage modifies this according to the gain coefficient:

$$V_{VFD\_Input} = V_{out\_DAC} \times \left(1 + \frac{R_f}{R_{in}}\right) = V_{out\_DAC} \times 2.0$$

This yields a linear 0-10 V reference vector. The VFD translates this input voltage into an output frequency line (F_{Out}) mapped between programmed operational boundaries
(F_{min} = 5 Hz, F_{max} = 50 Hz):

$$F_{Out} = F_{min} + \left(\frac{V_{VFD\_Input}}{10.0} \times (F_{max} - F_{min}) \right)$$

The theoretical synchronous speed of the rotating magnetic field (N) varies based on the number of stator magnetic poles (P = 4) and output frequency:

$$N_S = \frac{120f}{p}$$

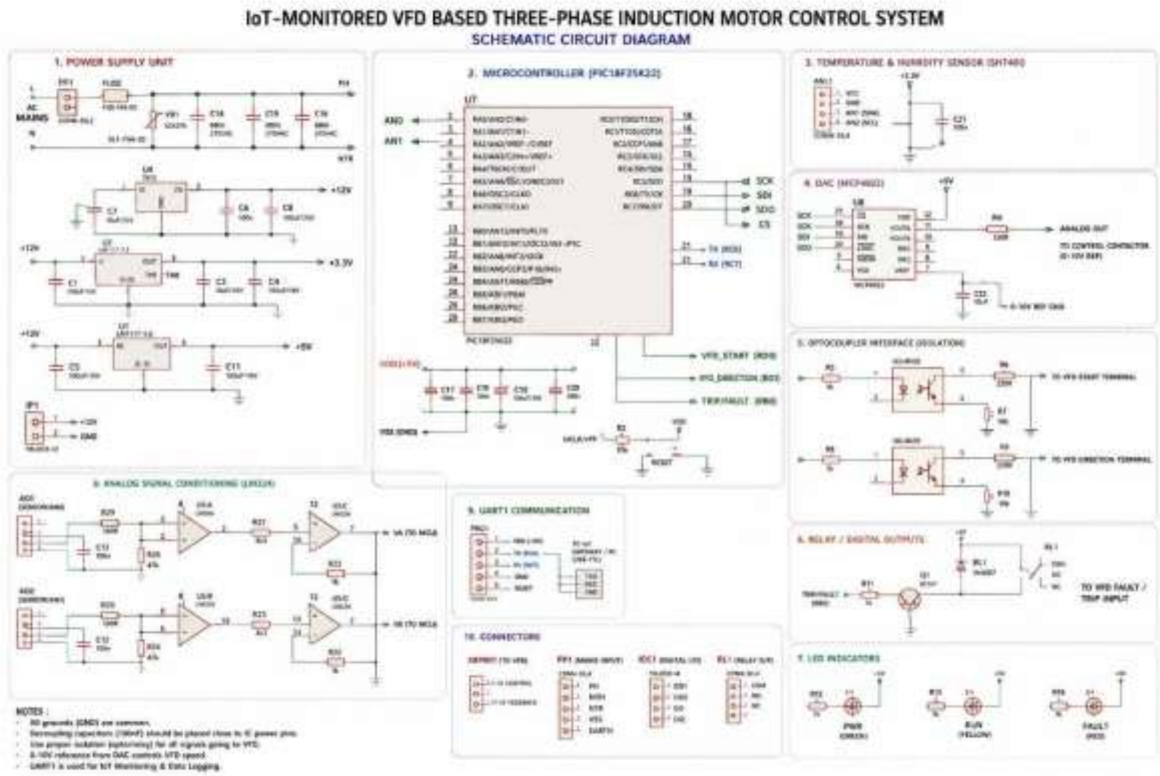

Figure 4.1: Schematic Circuit Diagram of The System

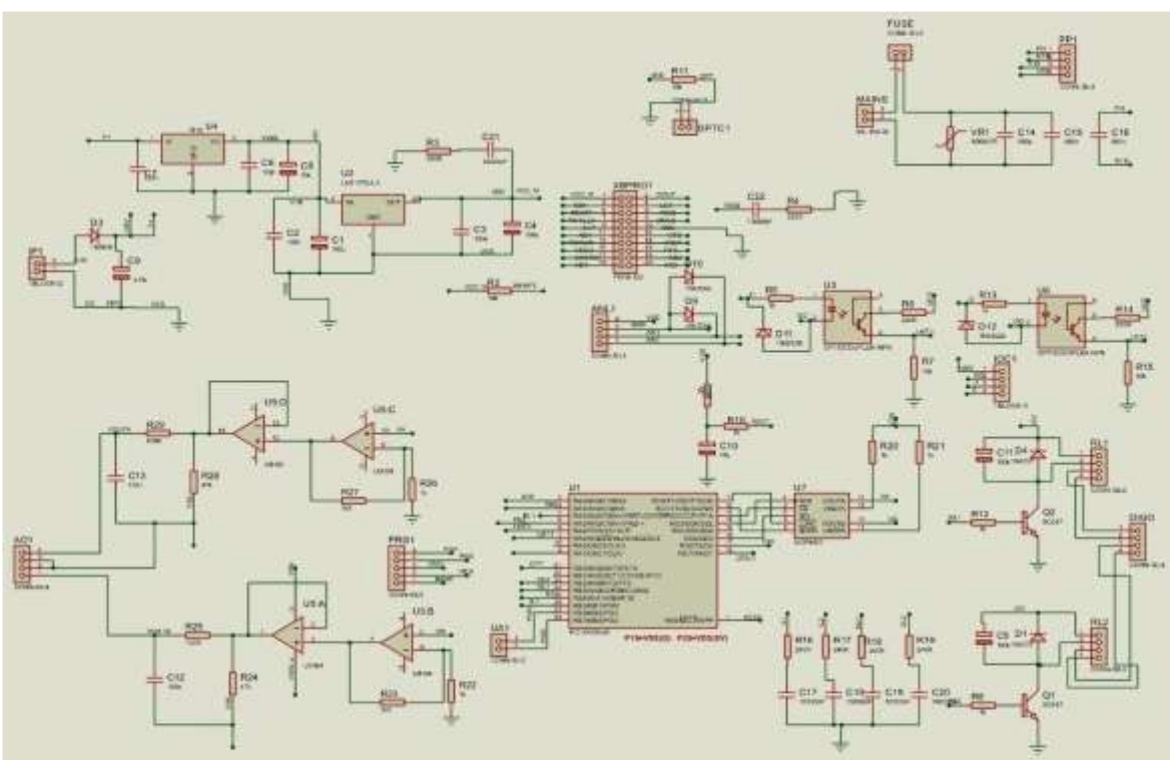

Figure 4.2 : PCB Layout of The System

B. Firmware Flow and Telemetry Stream

The firmware architecture was written in ANSI C using the XC8 compiler within the MPLAB X Integrated Development Environment. The software uses an interrupt-driven, non-blocking execution cycle to prevent processing delays from affecting the core motor safety monitoring loops.

Upon power-up or hardware reset events, the execution flow follows a sequential initialization routine as follows:

1) The internal oscillator registers (OSCCON, OSCCON2) enable the PLL block to establish a stable 64MHz processor clock.
2) The Data Direction Registers (TRIS) and Analog Select bits (ANSEL) allocate analog inputs to channels AN0 and AN1 while establishing digital outputs for the VFD gating commands.
3) The MSSP peripheral is initialized to SPI Master Mode 0,0, configuring the master clock to line frequencies optimal for the external DAC.
4) The EUSART engine sets up asynchronous UART data transfers at a transmission speed of 9600 baud with eight data bits, no parity check, and one stop bit (8N1 configuration).

Every 2 s, a hardware Timer1 overflow interrupt sets a data-logging flag, which serializes an ASCII message string formatted for external database parsing. The structural format uses a start delimiter ($), data identifiers, and a Carriage Return-Line Feed (\r\n) termination sequence

$MOTOR, TEMP: 28.4, HUM: 55.2, DRV: 60, STS : RUN\r\n

This stream passes through an HC-05 Bluetooth transceiver operating in the Serial Port Profile (SPP) transparent bridge mode at 2.4 GHz. An edge computer pairings maps this data into a virtual COM interface, where a Node-RED runtime routes telemetry to a graphical monitoring dashboard.

C. Experimental Hardware Setup

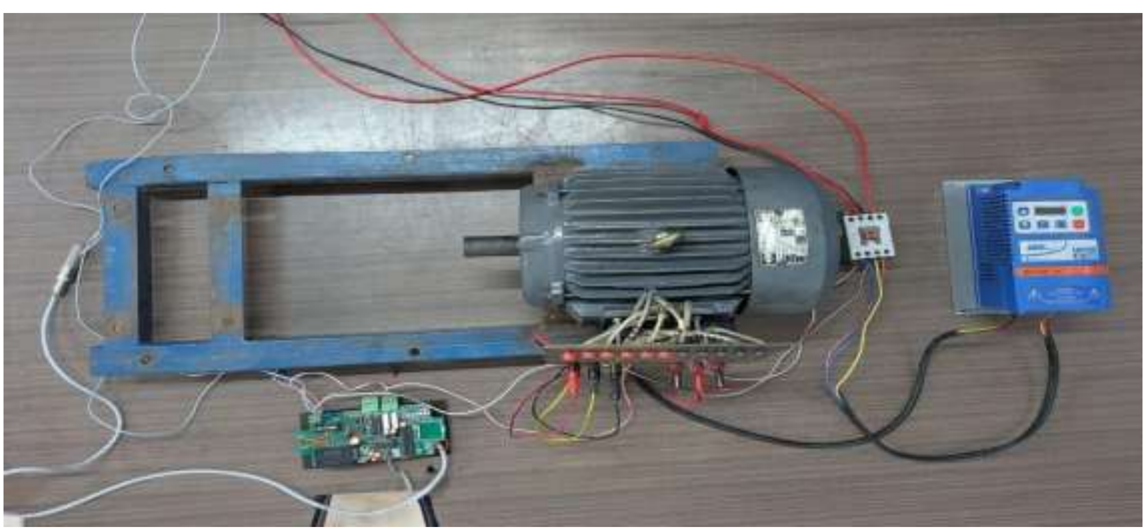

Figure 5.1 : Hardware Setup of The System

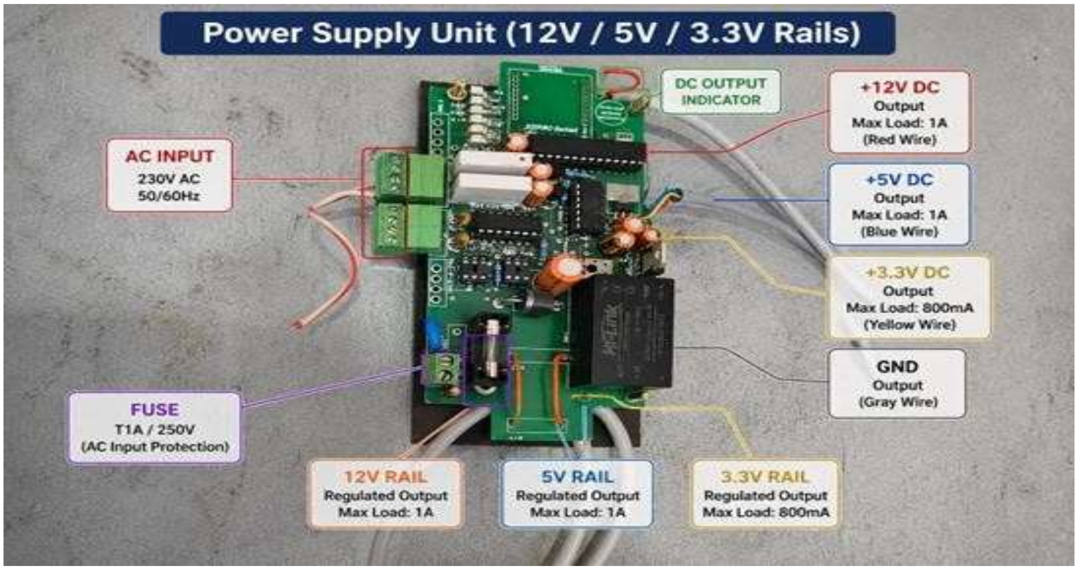

Figure 5.2 : Hardware Setup of The System

5. Results and Discussion

A. DAC Calibration and Precision Verification

To evaluate the voltage accuracy of the MCP4922 and non-inverting scaling stage, the system was programmed with 11 standardized test points. The output voltages were recorded at the scaled analog control terminals using a calibrated Fluke 87V True-RMS Digital Multimeter.

Speed %	Expected (V)	Measured (V)	Error (%)
0	0.000	0.002	N/A
10	1.000	0.998	0.20
20	2.000	2.001	0.05
30	3.000	2.998	0.07
40	4.000	4.003	0.08
50	5.000	4.999	0.02
60	6.000	5.997	0.05
70	7.000	7.002	0.03
80	8.000	7.998	0.03
90	9.000	9.004	0.04
100	10.000	9.997	0.03

Table 6.1 :DAC Output Voltage Accuracy Test Results

The data confirm that the output errors remain strictly within across the full dynamic range. The maximum absolute offset error was limited to 4mV, well below the standard VFD analog input step tolerance (This minimal variance guarantees smooth speed tracking and eliminates high-frequency noise injection into the control loop.

B. Motor Speed and Frequency Mapping Analysis

Shaft rotational speed metrics were verified using a handheld optical tachometer over designated target profiles , establishing a linear relationship with the generated frequency references.

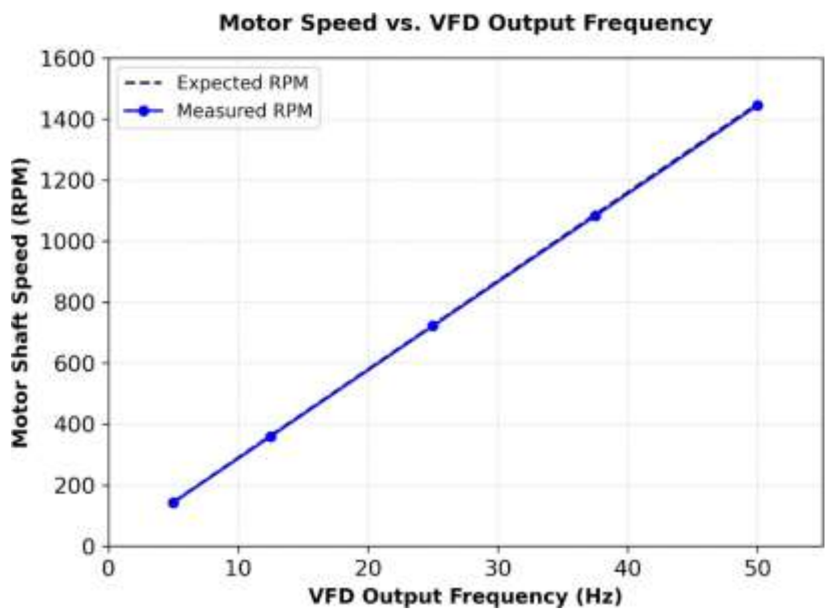

Figure 6.2. Graph of Motor Speed vs VFD Output Frequency

The induction motor tracked the linear *V/f* curve smoothly across the entire operational frequency range. Minor rotor slip accounted for the marginal difference between the theoretical synchronous metrics and the physical shaft readings, indicating high-fidelity transfer tracking.

C. Environmental Sensor Validation

The interfacing accuracy of the SHT40I was evaluated by placing the system inside an environmental chamber alongside a high-precision reference hygrometer.

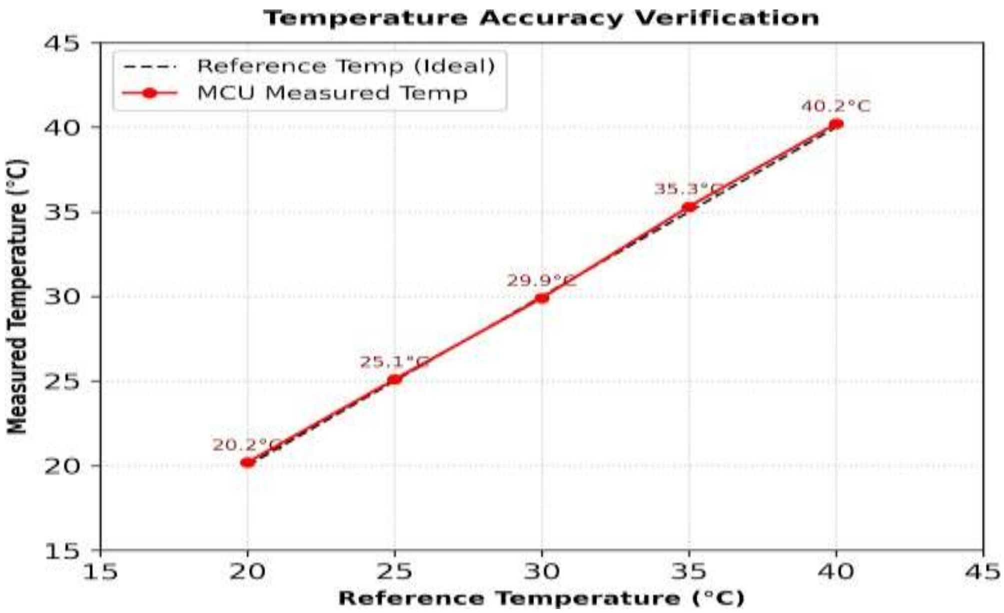

Figure 6.. Temperature Accuracy Verfication

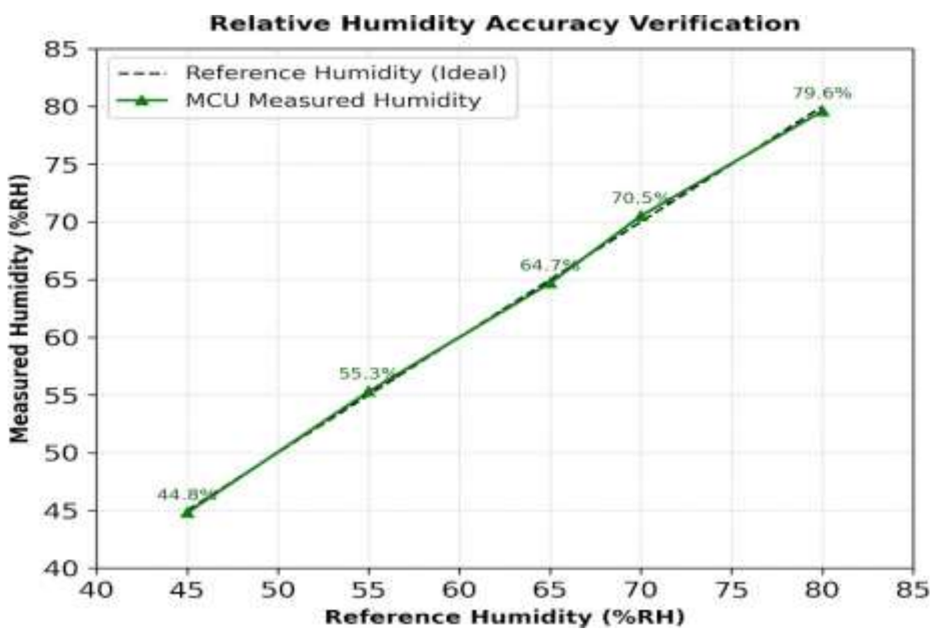

Figure 6.4 : Relative Humidity Accuracy Verification

Experimental variations were tightly bounded within a temperature tolerance envelope and humidity window. This accuracy confirms that the linear calibration scaling models implemented in the firmware are executed with high precision, enabling dependable automated system adjustments.

D. Telemetry Loop and Stress Endurance Testing

To verify communication reliability, a data integrity test was performed by linking the platform with a host processing application for an uninterrupted testing interval. Across 1,800 sequentially transferred packet bursts, zero framing dropouts and syntax parsing corruptions were registered. This confirms the stable synchronization using the internal clocking architecture.

The long-term thermal load capacity was evaluated by running the integrated assembly continuously for a 24-hour test period while varying the load between 40% and 90% at 30-minute intervals. Surface measurements showed that the control PCB temperature stabilized below in ventilated industrial housing. No watchdog timeout loops or reset exceptions were recorded, verifying the high operational reliability of the hardware design under continuous switching conditions.

6. Advantages and Applications

A. Technical Advantages

a) **Decentralized Optimization:** Shifting processing logic from complex industrial PLCs to low-cost microcontrollers significantly lowers installation and maintenance barriers while preserving high computing efficiency.

b) **High-Resolution Analog Tracking:** Implementing an isolated 12-bit SPI DAC enabled detailed analog adjustments down to single-millivolt increments. This eliminates the output voltage fluctuations that are common in traditional pulse width modulation low-pass filters.

c) **Integrated Protective Automation:** Native environmental tracking protects the drive electronics from high thermal stress by dynamically adjusting the cooling ventilation profiles before critical thresholds are reached.

d) **Reduced Mechanical Stress:** Setting adjustable acceleration and deceleration profiles minimizes the starting inrush currents and mechanical torque spikes, reducing the physical wear on the motor bearings and windings.

B. Target Deployments

a) **Smart Industrial Ventilation (HVAC):** Automated extraction fan arrays that dynamically scale extraction performance based on temperature and air quality measurements inside electrical enclosures.

b) **Pumping and Fluid Infrastructure:** Chemical processing installations requiring exact flow velocity scaling via frequency mapping while optimizing energy utilization.

c) **Conveyor Handling Networks:** Factory assembly networks requiring exact variable speed coordination linked with automated data logging systems for throughput tracking.

d) **Automated Cooling Towers:** Coolant fluid generation units requiring real-time fan modulation relative to seasonal humidity profiles and heat loads.

7. Conclusion and Future Scope

A. Conclusion

This paper details the design and deployment of a cost-effective, high-resolution microcontroller platform that provides localized intelligence and network telemetry to industrial motor drive automation. The combination of a PIC18F25K22 controller with a 12-bit SPI DAC enabled smooth, stable, and linear variable frequency motor speed adjustments. This architectural approach moves beyond basic on/off operations to deliver continuous and energy-efficient control profiles governed by fluid affinity laws.

Experimental testing confirmed that the scaled analog voltage outputs maintained a tight accuracy profile within the error margins. In addition, the hardware telemetry loop achieved complete reliability across long-term testing intervals without packet degradation. The integration of real-time environmental tracking enables robust protective responses, establishing the design as a viable, low-cost, decentralized alternative to classic PLC configurations in modern smart manufacturing frameworks.

B. Future Scope

Although the current implementation meets its baseline design objectives, future enhancements will focus on expanding industrial durability.

a) **Global Networking Upgrades: :** Replacing local short-range modules with dual-band WiFi /cellular transceivers to enable edge-to-cloud parameter ingestion across broad factory landscapes.
b) **Standard Industrial Bus Integration:** Rewriting the peripheral firmware layer to support differential Modbus RTU protocols over RS-485 physical links, enabling drop-in compatibility with legacy industrial automation networks.
c) **Predictive Diagnostics via Edge ML:** Deploying lightweight machine learning anomaly classification algorithms directly onto localized edge hardware to identify early insulation degradation or bearing wear based on historical vibrations and current profiles.
d) **Integrated Power Quality Monitoring:** Integration of precision multichannel energy analyzer ICs to enable direct tracking of real-time power factor metrics and total harmonic distortion (THD) characteristics.

References

[1] M. M. Siddiqui, A. S. A. Hadhri, A. S. H. A. Kathir, and A. A. Alnajjar, "Integrated Real-Time Monitoring of Three-Phase Induction Motors," *Journal of Physics: Conference Series*, vol. 3191, no. 1, p. 012001, 2026.

[2] G. Anbarasi, "Advanced Control and Protection of Three-Phase Induction Motors for Industrial Automation," in *Proceedings of the 4th International Conference on Innovative Mechanisms for Industry Applications (ICIMIA)*, Sep. 2025, pp. 32–38.

[3] P. Shaw, N. K. Sharma, and B. Patnaik, "Induction Motors with Variable Frequency Drives: A Systematic Review with Focus on Health Monitoring," in *Proceedings of the IEEE North-East India International Energy Conversion Conference and Exhibition (NE-IECCE)*, Jul. 2025, pp. 1– 6.

[4] N. R. Putri, M. Yuhendri, "Three-phase induction motor control using scalar control method based on the Internet of Things (IoT)," *Journal of Industrial Automation and Electrical Engineering*, vol. 2, no. 2, pp. 29–35, 2025.

[5] S. Buwarda, Mutmainnah, and M. F. Yakob, "Design and Development of a Three-Phase Induction Motor Speed Control System Using Altivar 61 Based on Temperature Sensor and Internet of Things (IoT)," *Jurnal Teknologi Elekterika*, vol. 22, no. 2, pp. 60–64, 2025.

[6] A. Marzuki, T. Muzakkir, and M. S. Arief, "Three-Phase Induction Motor Control and Monitoring Using VFD and ESP32 Based on Modbus RTU Protocol," *American Journal of Electrical and Computer Engineering*, vol. 8, no. 2, pp. 71–80, 2024.

[7] U. Syarah and M. Yuhendri, "Constant Torque Control of Induction Motor Using Variable Frequency Drive Based on Internet of Things," *Journal of Industrial Automation and Electrical Engineering*, vol. 1, no. 1, pp. 7–12, Jul. 2024.

[8] D. Kalel and R. R. Singh, "IoT integrated adaptive fault tolerant control for induction motor based critical load applications," *Engineering Science and Technology, an International Journal*, vol. 51, p. 101585, 2024.

[9] C. Kiriella and N. Kulasooriya, "A Low Cost Three Phase Induction Motor Drive for Single Phase Fed Industries," in *Proceedings of the 2022 International Conference on Electrical, Computer and Energy Technologies (ICECET)*, 2022, pp. 1–6.

[10] M. A. Aiman, A. H. Hussian, M. T. Ibrahim, and S. Pambudi, "IoT Implementation Based on Power Quality Network Analyzer for 3-Phase Induction Motor Control," *Teknika*, vol. 10, no. 2, pp. 46–56, 2021.

[11] R. Sureshkumar, Prasad, S.S., Karthikeyan, G., Kumar, C.P. and Pravina, S.V., "Three phase induction motor position control using V20 drive," *AIP Conference Proceedings*, vol. 2387, no. 1, p. 140022, Nov. 2021.

[12] D. Chaudhary and R. Mehta, "IoT based Conditioning Monitoring of Motor with the help of Variable Frequency Drive," in *Proceedings of the Recent Advances in Renewable Energy Sources (RARES2021)*, 2021.

[13] R. Jyothi, K. U. Rao and R. Jayapal, "IoT application for real-time condition monitoring of voltage source inverter driven induction motor," in *Innovative Data Communication Technologies and Application: Proceedings of ICIDCA 2020*, Singapore: Springer, 2021, pp. 97–105.

[14] S. Bodke, D. Patil, R. Salgar, and D. N. Ghuge, "Application of VFD For Three Phase Induction Motor," in *Proceedings of the 2nd International Conference on Communication & Information Processing (ICCIP)*, Mar. 2020.

[15] *Sensirion AG*, "SHT4x Datasheet: Humidity and Temperature Sensor," Staefa, Switzerland, 2021.